Membrane-shaping host reticulon proteins play crucial roles in viral RNA replication compartment formation and function

Arturo Diaz[a], Xiaofeng Wang[a,1], and Paul Ahlquist[a,b,2]

[a]Institute for Molecular Virology and [b]Howard Hughes Medical Institute, University of Wisconsin, Madison, WI 53706

Contributed by Paul Ahlquist, July 29, 2010 (sent for review May 14, 2010)

Positive-strand RNA viruses replicate their genomes on membranes with virus-induced rearrangements such as single- or double-membrane vesicles, but the mechanisms of such rearrangements, including the role of host proteins, are poorly understood. Brome mosaic virus (BMV) RNA synthesis occurs in ≈70 nm, negatively curved endoplasmic reticulum (ER) membrane invaginations induced by multifunctional BMV protein 1a. We show that BMV RNA replication is inhibited 80–90% by deleting the reticulon homology proteins (RHPs), a family of membrane-shaping proteins that normally induce and stabilize positively curved peripheral ER membrane tubules. In RHP-depleted cells, 1a localized normally to perinuclear ER membranes and recruited the BMV 2a^{pol} polymerase. However, 1a failed to induce ER replication compartments or to recruit viral RNA templates. Partial RHP depletion allowed formation of functional replication vesicles but reduced their diameter by 30–50%. RHPs coimmunoprecipitated with 1a and 1a expression redirected >50% of RHPs from peripheral ER tubules to the interior of BMV-induced RNA replication compartments on perinuclear ER. Moreover, RHP-GFP fusions retained 1a interaction but shifted 1a-induced membrane rearrangements from normal vesicles to double membrane layers, a phenotype also induced by excess 1a-interacting 2a^{pol}. Thus, RHPs interact with 1a, are incorporated into RNA replication compartments, and are required for multiple 1a functions in replication compartment formation and function. The results suggest possible RHP roles in the bodies and necks of replication vesicles.

positive-strand RNA virus | reticulons | genomic RNA replication complex | endoplasmic reticulum vesicles

A universal feature of (+)RNA viruses is that they replicate their RNA on intracellular membranes, usually in association with vesiculation or other membrane rearrangements (1–3). As a highly conserved feature of (+)RNA virus life cycles, such membrane involvement is a potentially valuable target for broad-spectrum antiviral treatments.

Brome mosaic virus (BMV) is a member of the alphavirus-like superfamily of human, animal, and plant viruses. BMV encodes two RNA replication proteins. BMV 1a contains an N-proximal domain with m^7G methyltransferase and covalent m^7GMP-binding activities required for viral RNA capping (4–6), and a C-terminal NTPase/RNA helicase-like domain (7). BMV 2a^{pol} has a central RNA-dependent RNA polymerase-like domain and an N-terminal domain that interacts with the 1a helicase domain (8, 9). In both the yeast *Saccharomyces cerevisiae* and its natural plant hosts, BMV RNA is selectively encapsidated into progeny virions (10), and BMV RNA replication depends on 1a, 2a^{pol} and specific *cis*-acting RNA signals (11), localizes to ER membranes (12, 13), generates a dramatic excess of positive- to negative-strand RNA (14), and efficiently directs subgenomic mRNA synthesis (14).

BMV 1a localizes to perinuclear ER membranes and induces 60- to 75-nm vesicular invaginations or spherules. BMV 1a's high multiplicity in spherules (15), strong membrane association (16), and self-interaction (17) imply that 1a may induce spherule invagination away from the cytoplasm (negative membrane curvature) by forming a capsid-like shell on the spherule interior (15). In the presence of low levels of 2a^{pol} and a viral RNA template, spherules serve as compartments or mini-organelles for RNA replication (15). Many other (+)RNA viruses, including flaviviruses (18), nodaviruses (3) and alphaviruses (19), also replicate in association with ≈50- to 80-nm-diameter spherules. However, for BMV, increasing 2a^{pol} levels shift the spherular membrane rearrangements to large multilayer stacks of appressed double-membrane layers that, like spherules, are the sites of 1a and 2a^{pol} accumulation, protect RNA templates from nucleases, and support RNA replication (20).

The mechanisms by which (+)RNA viruses induce and maintain such membrane rearranged RNA replication compartments and the role of host factors in this process are not resolved. Here, we reveal and dissect the critical roles of the reticulon homology domain proteins (RHPs) in BMV RNA replication compartment formation and function. The RHPs are a family of membrane-shaping proteins conserved from yeast to humans and plants (21, 22). RHPs share similar ≈200-aa domains with two long hydrophobic segments that insert in the cytoplasmic face of membranes to induce positive membrane curvature (protrusion toward the cytoplasm). RHPs primarily partition to and stabilize positively curved peripheral ER membrane tubules while avoiding the low-curvature ER domains of the nuclear envelope and peripheral ER sheets (23–28). Genome-wide deletion analysis in yeast, which encodes three RHPs (Rtn1p, Rtn2p, and Yop1p), previously revealed only a 2-fold reduction in BMV replication on deleting Rtn1p and just a ≈10–20% reduction on deleting Rtn2p or Yop1p, respectively (29). However, we show that 1a interacts with RHPs and relocalizes them from peripheral ER tubules to the interior of the spherular BMV RNA replication compartments. Moreover, consistent with the RHPs' redundant roles in the cell (25), simultaneously deleting Rtn1p and Yop1p or all three RHPs severely inhibited BMV RNA replication, abolished 1a-induced spherule formation and altered the number and morphology of 1a-induced double-membrane layers, whereas GFP-tagged versions of the RHPs prevented spherule formation. These and other results show that the RHPs play important roles in the formation and function of BMV-induced replication compartments.

Results

Deleting RHP Genes Inhibits BMV RNA Replication. BMV 1a by itself or with low levels of 2a^{pol}, expressed from the *ADH1* promoter, induces spherular ER invaginations, whereas 1a plus high 2a^{pol}

Author contributions: A.D., X.W., and P.A. designed research; A.D. performed research; A.D. contributed new reagents/analytic tools; A.D., X.W., and P.A. analyzed data; and A.D. and P.A. wrote the paper.

The authors declare no conflict of interest.

[1]Present address: Texas AgriLife Research and Department of Plant Pathology and Microbiology, Texas A&M University System, Weslaco, TX 78596.

[2]To whom correspondence should be addressed. E-mail: ahlquist@wisc.edu.

This article contains supporting information online at www.pnas.org/lookup/suppl/doi:10.1073/pnas.1011105107/-/DCSupplemental.

levels, driven by the *GAL1* promoter, induce stacked layers of double-membrane ER (15, 20). To assess the role of RHPs in BMV RNA replication, we measured positive- and negative-strand subgenomic RNA4 accumulation in wt, single- (*rtn1*Δ, *rtn2*Δ, or *yop1*Δ), and double-knockout (*rtn2*Δ*yop1*Δ or *rtn1*Δ*yop1*Δ) yeast expressing 1a, RNA3, and *ADH1* $2a^{pol}$ or *GAL1* $2a^{pol}$. Wt yeast cells supported high levels of positive-strand RNA3 and subgenomic RNA4 in both spherules and layers (Fig. 1, lane 1). *rtn2*Δ, *yop1*Δ, and *rtn2*Δ*yop1*Δ yeast also supported RNA4 synthesis to wt levels (Fig. 1, lanes 3–5). *rtn1*Δ yeast supported RNA4 synthesis to 53% and 58% of wt levels in spherules and layers, respectively (Fig. 1, lane 2). Moreover, in *rtn1*Δ*yop1*Δ yeast, RNA4 synthesis was inhibited by 92% and 67% in spherules and layers, respectively (Fig. 1, lane 6). A similar trend was observed for negative-strand RNA synthesis (Fig. S1*A*). Although *rtn1*Δ*yop1*Δ yeast grew at ≈2/3 the wt rate, general transcription and translation were not affected (e.g., Fig. 1, see 18S RNA; Fig. S1 see Pgk1 levels). Consistent with their overlapping functions, the separate and additive effects of the RHP gene deletions on BMV mirror their relative expression levels of Rtn1p > Yop1p > Rtn2p (30).

The above yeast deletion mutants were made in *S. cerevisiae* strain YPH500, used in most past studies of BMV RNA replication (12, 15, 20, 31). Despite extensive efforts, we could not generate YPH500 *rtn1*Δ*rtn2*Δ or *rtn1*Δ*rtn2*Δ*yop1*Δ strains, suggesting that these deletions inhibit cell growth in the YPH500 background. However, for widely used strain BY4741, which also has been used to study many aspects of BMV replication (29, 32), an *rtn1*Δ*rtn2*Δ*yop1*Δ triple knockout strain has been generated (25). This mutant has no growth defect, and ER morphology changes caused by RHP deletion do not block vesicular trafficking out of the ER (25). In *rtn1*Δ*rtn2*Δ*yop1*Δ yeast, positive-strand RNA4 accumulation decreased by 80% and 90% in spherules and layers compared with their levels in wt BY4741 yeast (Fig. 1, lanes 7 and 8). Hereafter, results described for single- and double-knockouts were based on YPH500 derivatives, whereas *rtn1*Δ*rtn2*Δ*yop1*Δ yeast were on the BY4741 background.

Moreover, 1a and $2a^{pol}$ levels were not altered in the absence of RHPs, ruling out the possibility that the decrease in RNA replication might be due to a destabilizing effect on the viral replicase proteins (Fig. S1 *B* and *C*). Additionally, 1a and $2a^{pol}$ localized normally to the perinuclear ER in most strains (Fig. S2). However, in *rtn1*Δ*rtn2*Δ*yop1*Δ yeast-expressing layers, only a portion of 1a was associated with the perinuclear ER, whereas the majority of 1a colocalized with Sec63 in aberrant regions of ER that extended away from the nucleus (Fig. S2*C*).

Deleting RHPs Reduces Spherule Numbers and Diameter. To determine whether spherule formation or structure was affected by RHP deletion, we measured the abundance and diameter of spherules in the subset of cells that were sectioned through their nuclei among a total of 200 cells for each strain. In wt and *rtn2*Δ yeast, the average spherule diameter was 58–74 nm, whereas in *yop1*Δ, *rtn1*Δ, and *rtn2*Δ*yop1*Δ yeast, spherules averaged 48, 35, and 27 nm in diameter, respectively (Fig. 2 *A–C* and Fig. S3). For *rtn2*Δ*yop1*Δ yeast in particular, the >2-fold decrease in spherule diameter was paralleled by a >2-fold increase in spherule frequency (Fig. 2*C*), possibly reflecting the unchanged level of spherule-lining 1a protein (Fig. S1). Finally, in *rtn1*Δ*yop1*Δ and *rtn1*Δ*rtn2*Δ*yop1*Δ yeast, spherules were not detected among thousands of cells examined (Fig. 2*C*).

In yeast cells, the half-life of RNA3 increases from 5 to 7 min in the absence of 1a to >3 h in the presence of 1a, which is reflected in a marked increase in RNA3 accumulation (33). This 1a-induced, stabilized state is consistent with RNA3 relocation to the interior of the 1a-induced spherules (15). In wt, single-deletion, and *rtn2*-Δ*yop1*Δ yeast, 1a increased RNA3 accumulation 8- to 11-fold over that in cells lacking 1a (Fig. S4). However, in *rtn1*Δ*yop1*Δ yeast, RNA3 accumulation did not increase in the presence of 1a (Fig. S4). Thus, Rtn1p and Yop1p in particular modulate the formation and size of 1a-induced membrane spherules.

Deleting RHPs Alters Number and Morphology of Double-Membrane Layers. Electron micrographs of wt yeast expressing 1a plus *GAL1* $2a^{pol}$ showed a series of 2–5 appressed layers of double-membrane ER surrounding the nucleus (Fig. 3*A*). Likewise, multiple double-membrane layers were found in *rtn1*Δ (Fig. 3*B*), *rtn2*Δ, *yop1*Δ, and *rtn2*Δ*yop1*Δ yeast (Fig. S3). *rtn1*Δ*yop1*Δ and *rtn1*Δ*rtn2*Δ*yop1*Δ yeast, in which RNA replication was inhibited by 70–90% (Fig. 1), predominantly had only a single double-membrane layer surrounding the nucleus (Fig. 3 *C* and *D*). Moreover, simultaneously deleting the three RHPs disrupted the normal close pairing of adjacent double-membrane layers, leading to dramatic bulges in the normally regular, narrow interlayer space (Fig. 3*D*), reminis-

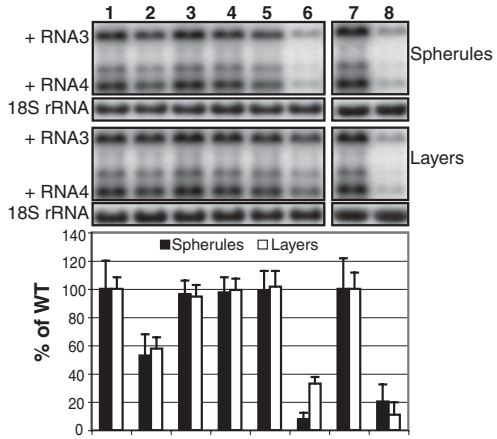

Fig. 1. BMV RNA replication is inhibited in specific reticulon deletion yeast strains. Total RNA extracts were obtained from wt YPH500 (lane 1), *rtn1*Δ (lane 2), *rtn2*Δ (lane 3), *yop1*Δ (lane 4), *rtn2*Δ*yop1*Δ (lane 5), *rtn1*Δ*yop1*Δ (lane 6), wt BY4741 (lane 7), or *rtn1*Δ*rtn2*Δ*yop1*Δ (lane 8) yeast coexpressing 1a, RNA3, and either *ADH1* $2a^{pol}$ (Spherules) or *GAL1* $2a^{pol}$ (Layers), and accumulation of RNA3 and subgenomic RNA4 was detected by Northern blotting. Equal loading was verified by probing for 18S ribosomal RNA. Values represent the mean of three independent experiments.

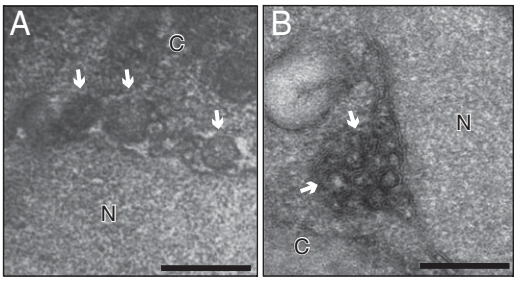

C

Strain	Avg. Diameter	Spherules/Cell
WT	74 ± 16 nm	5.5
*rtn1*Δ	34 ± 9 nm	6.6
*rtn2*Δ	58 ± 9 nm	6.4
*yop1*Δ	48 ± 9 nm	7.33
*rtn2*Δ*yop1*Δ	27 ± 4 nm	14.5
*rtn1*Δ*yop1*Δ	ND	0
*rtn1*Δ*rtn2*Δ*yop1*Δ	ND	0

Fig. 2. BMV-induced spherule formation is abolished in the absence of RHPs. Representative EM images of wt (*A*) and *rtn1*Δ (*B*) yeast cells expressing BMV-induced spherules. White arrows point out individual spherular structures. N, nucleus; C, cytoplasm. (Scale bars: 200 nm.) (*C*) Effect of RHP deletion on spherule diameter and number of spherules per cell.

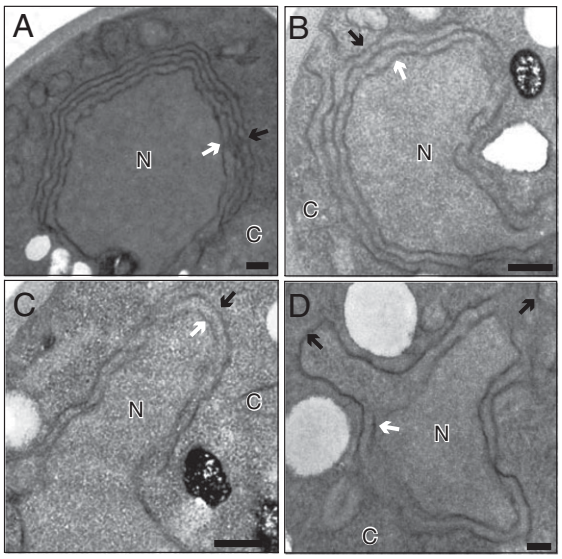

Fig. 3. Morphology and number of double-membrane layers is altered in triple and one double deletion strain. EM images of yeast cells expressing BMV induced layers in wt (*A*), *rtn1*Δ (*B*), *rtn1*Δ*yop1*Δ (*C*), or *rtn1*Δ*rtn2*Δ*yop1*Δ (*D*) yeast. Black arrows point out double-membrane layers, whereas white arrows point out the nuclear membrane. N, nucleus; C, cytoplasm. (Scale bars: 200 nm.)

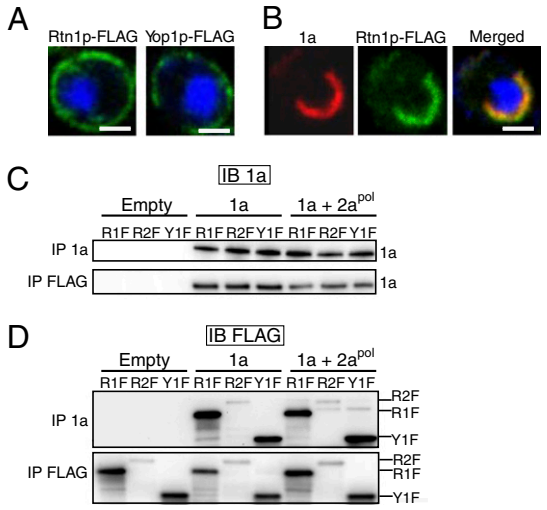

Fig. 4. RHPs interact with BMV 1a protein and relocalize to site of BMV replication. Localization of FLAG-tagged RHPs in yeast transformed with empty plasmids (*A*) or 1a alone (*B*). DNA was stained with DAPI (blue). Images were cropped just outside the yeast cell wall to include only one cell. (Scale bars: 2 μm.) (*C* and *D*) Cells expressing the FLAG-tagged RHPs and either empty plasmids, 1a alone, or 1a plus *GAL1* $2a^{pol}$ were lysed, and the cleared lysates were subjected to immunoprecipitation by using anti-1a or anti-FLAG antibodies (IP 1a and IP FLAG, respectively). The resulting immunoprecipitates were analyzed on 4–15% SDS/PAGE and immunoblotted using anti-1a (*C*) or anti-FLAG (*D*) antibodies. The positions of 1a, Rtn1p-FLAG (R1F), Rtn2p-FLAG (R2F), and Yop1p-FLAG (Y1F) are shown on the right.

cent of the aberrant regions of ER seen by using confocal microscopy (Fig. S2*C*).

Because many lipid synthesis steps occur on smooth tubular ER (34) shaped by RHPs (25, 26, 35), it seemed possible that RHP depletion might affect these steps, perhaps explaining why spherule and normal double-membrane layer formation were suppressed in *rtn1*Δ*yop1*Δ and *rtn1*Δ*rtn2*Δ*yop1*Δ yeast. However, total lipid levels and the major fatty acid species in *S. cerevisiae*, palmitic acid (16:0), stearic acid (18:0), palmitoleic acid (16:1), and oleic acid (18:1) in wt and *rtn1*Δ*rtn2*Δ*yop1*Δ yeast expressing either spherules or layers were not significantly changed (Fig. S5). Therefore, the decreased number of double-membrane layers in *rtn1*Δ*yop1*Δ and *rtn1*Δ*rtn2*Δ*yop1*Δ yeast was not due to a change in total lipid levels or lipid composition.

BMV 1a Interacts with and Relocalizes RHPs to BMV RNA Replication Sites. Because the ER membrane-shaping RHPs were required to form BMV-induced spherules and normal double-membrane layers, we examined the localization of FLAG-tagged Rtn1p and Yop1p expressed from their endogenous promoters. Consistent with previous reports, RHPs were almost absent from the nuclear envelope but were abundant in the peripheral ER (Fig. 4*A*) (25), which in yeast is located primarily beneath the plasma membrane (36). In contrast, in yeast expressing 1a alone or with $2a^{pol}$ (Fig. 4*B*), the majority of RHPs colocalized with 1a in the perinuclear ER (12, 13).

Next, we used immunoprecipitation (IP) to determine whether 1a interacted with the RHPs. Western blotting showed that after IP with anti-FLAG antibody, 1a was detected in yeast coexpressing FLAG-tagged RHPs and 1a or 1a plus $2a^{pol}$, but not in yeast lacking 1a (Fig. 4*C Lower*) or expressing 1a but not FLAG-tagged RHPs. Similarly, after IP with anti-1a antibody, Rtn1p-, Rtn2p-, and Yop1p-FLAG were strongly detected (Fig. 4*D Upper*). IP with anti-FLAG antibody and immunoblotting for FLAG confirmed that the RHP-FLAG proteins were expressed (Fig. 4*D Lower*).

A control IP confirmed that $2a^{pol}$-GFP, which like wt $2a^{pol}$ interacts with 1a (8, 9), immunoprecipitated with 1a, whereas free GFP and Sec63-GFP, a transmembrane ER protein, did not (Fig. S6*B*). Moreover, RHPs did not co-IP with $2a^{pol}$ in the absence of 1a (Fig. S6*A*). Together, the results indicate that RHPs are recruited to or retained at BMV RNA replication sites through a specific interaction with 1a.

RHPs Localize to Interior of Spherules and Double-Membrane Layers. To more precisely localize RHPs in relation to BMV-induced replication compartments, we performed immunogold EM with an antibody recognizing FLAG-tagged RHPs and a secondary antibody conjugated to gold particles. The need to reduce osmium treatment to preserve antigenicity reduced direct membrane staining but, as in prior studies (15, 20), spherules remained readily recognizable by the electron lucence of their bounding membranes and high electron density of their interior contents relative to general cytoplasm (Fig. 5 *A* and *B*). Of >100 gold particles examined in the absence of BMV components, only ≈7% were on or near the perinuclear ER (Fig. 5*E*). In cells expressing 1a, ≈55% of RHP-targeted gold particles were inside the ≈70 nm spherules (Fig. 5 *B* and *E*) or well within the ≈20 nm distance spanned by the primary and secondary antibodies (37). Likewise, in cells expressing 1a plus *GAL1* $2a^{pol}$, ≈57% of gold particles were on the double-membrane ER layers or in the cytoplasmically connected spaces between layers (Fig. 5 *D* and *E*). Notably, as integral membrane proteins inserted in the ER membrane cytoplasmic face (25), RHPs cannot be in the ER lumen. Thus, RHPs localize to the interior of spherules and double-membrane layers, where 1a also localizes (15, 20).

Fusing GFP to RHPs Shifts Spherules to Double-Membrane Layers. The small 8-aa FLAG tag used in previous experiments did not interfere with the normal localization of RHPs (Fig. 4*A*) and had no adverse effect on the formation and morphology of BMV-induced spherules and double-membrane layers (Fig. 5). However, we found that RHP-GFP fusions prevented spherule formation and instead formed a layer-like structure under conditions that normally produce spherules (Fig. S7*B*). The GFP-tagged RHPs relocalized from peripheral to perinuclear ER in the presence of 1a or 1a plus *GAL1* $2a^{pol}$ (Fig. S7 *C* and *D*) and co-IP

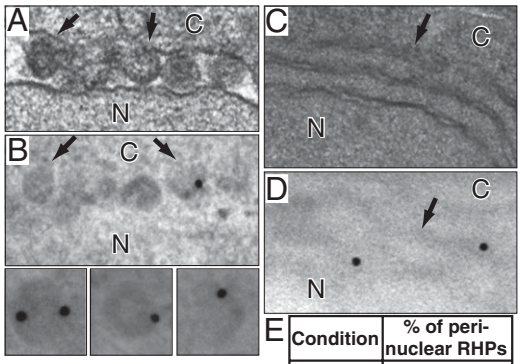

E

Condition	% of perinuclear RHPs
No BMV	7.5 ± 4.5
Spherules	55.0 ± 7
Layers	57.0 ± 8

Fig. 5. RHPs localize to interior of spherules and layers. EM images of osmium fixed yeast cells containing spherules (*A*) or layers (*C*). Anti-FLAG immunogold EM labeling in yeast cells expressing Rtn1p-FLAG and 1a (*B*) or 1a plus *GAL1* $2a^{pol}$ (*D*). Insets in *B* show individual spherules. To preserve the antigenicity of the proteins, osmium fixation and staining were reduced, resulting in electron lucent regions where the lipid membranes used to be due to lipid extraction during the dehydration steps. N, nucleus; C, cytoplasm. (*E*) Percentage of total gold particles that localized to perinuclear ER in yeast expressing no BMV components, spherules, or layers.

with 1a (Fig. S6*C*). Thus, RHPs are necessary to form spherular compartments as a GFP tag prevented formation of spherules while not interfering with RHP–1a interaction.

Discussion

To replicate their genomic RNAs, (+)RNA viruses induce membrane rearrangements that create membrane-linked RNA replication compartments, but how such rearrangements are accomplished remains largely unknown. Our results show that the membrane-shaping host RHPs localize to the sites of BMV RNA synthesis through an interaction with viral replication factor 1a, play crucial roles in BMV RNA synthesis, and are essential for forming the membrane-bounded replication compartments in which RNA synthesis occurs.

RHP Roles in Replication Vesicle Formation and Function. Previous work demonstrated that 1a membrane association and 1a–$2a^{pol}$ interaction precedes, and is independent of, membrane rearrangement (7, 31). Here, our data show that RHP deletion did not reduce 1a localization to ER membranes (Fig. S2) or 1a interaction with BMV $2a^{pol}$ (Fig. S2*D*). However, deleting all three RHP genes (*rtn1Δrtn2Δyop1Δ*) or the two most highly expressed RHP genes (*rtn1Δyop1Δ*) inhibited RNA replication 10-fold (Fig. 1) and abolished 1a-induced spherule formation (Fig. 2*C*) and viral RNA template protection (Fig. S4). This failure to protect viral RNAs may be due to not forming spherules. Prior results indicate that these vesicle interiors are the protected site in which 1a sequesters viral RNAs (7, 15) and, upon 1a mutation, increases and decreases in spherule formation and RNA template protection are closely correlated (31).

BMV 1a strikingly localized more than one-half of RHPs to the perinuclear ER and incorporated them inside the replication vesicles (Figs. 4 and 5). A challenge in understanding how RHPs contribute to spherule formation is that although 1a-induced spherules are invaginated away from the cytoplasm, RHPs pull ER membranes to protrude into the cytoplasm. Thus, superficially, it appears that RPH and 1a action should be antagonistic, not cooperative. However, RHPs also are involved in forming nuclear pores (38), which are topologically equivalent to spherule necks: both are positively curved channels from the perinuclear ER into the cytoplasm. Thus, one important role for RHPs may be stabilizing spherule necks (Fig. 6*A*). Because no membrane breakage is involved, every degree of negative curvature induced by 1a must be compensated by corresponding positive curvature at the neck. Consistent with such a role, RHPs polymerize into short arcs and need to occupy only ≈10% of a membrane surface to form tubules (35). Without RHPs to stabilize neck formation, 1a may not be able to progress beyond initial membrane deformation to make a full vesicle.

RHP expression levels and density on membranes vary the rate of bending and, thus, the diameter of ER tubules (35). Similar considerations may explain why partial RHP depletion in *rtn1Δ*, *yop1Δ*, and *rtn2Δyop1Δ* yeast reduced spherule diameter ≈2-fold (Fig. 2). Our 1a-RHP co-IP and immunogold results (Figs. 4 and 5) suggest that RHPs also may be incorporated with 1a into the main vesicle body (Fig. 6*A*). There, local positive curvature induced by membrane insertion of wedge-shaped RHPs should partially cancel negative curvature induced by adjacent 1a proteins, causing the membrane to bend toward closure more slowly and increasing spherule diameter relative to a pure 1a shell (Fig. 6*B*).

Notably, the smaller spherules supported substantial levels of RNA replication (Fig. 1). Thus, as long as large or small 1a-induced spherules formed, viral RNA templates were stabilized (Fig. S4) and replicated (Fig. 1), suggesting that a major RNA replication defect in *rtn1Δyop1Δ* and *rtn1Δrtn2Δyop1Δ* yeast was the failure to form replication compartments.

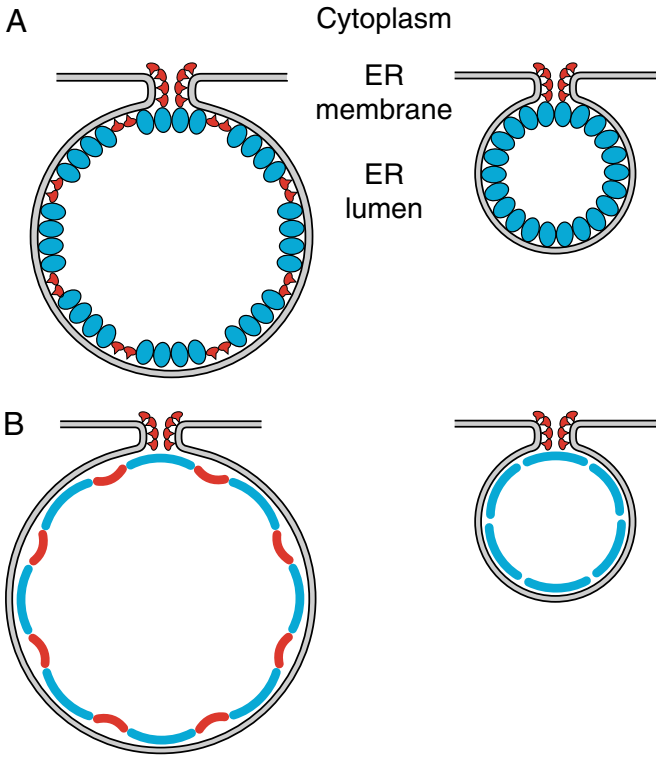

Fig. 6. Models for the potential role of RHPs in the formation and/or maintenance of BMV-induced spherules. (*A*) Schematic of BMV spherules showing how 1a (blue) might induce and stabilize negative membrane curvature in the vesicle body, whereas arced RHP multimers (red) might stabilize the positively curved neck region and also be incorporated in the main vesicle body. (*B*) Schematics replacing 1a and RHP clusters in the main vesicle body with blue and red arcs, respectively, to show how expansion of the vesicle body in RHP-containing spherule A is primarily due to the action of RHPs in partially neutralizing the intrinsic rate of membrane curvature by 1a alone.

RHP Roles in Double Membrane Layers. RHPs also were crucial for RNA replication under conditions of high $2a^{pol}$ expression, which shift 1a-induced replication compartments from vesicles to stacked double-membrane layers (20). RHP depletion in *rtn1*Δ, *rtn1*Δ*yop1*Δ, and *rtn1*Δ*rtn2*Δ*yop1*Δ yeast progressively inhibited layer formation and deranged layer morphology in parallel with inhibiting RNA replication (Figs. 1 and 4). Just as they stabilize ER tubules, RHPs might help to initiate each new layer by forming arc-like scaffolds to stabilize the positively curved ends (half tubules) where each perinuclear ER layer folds over to begin the next outer layer (Fig. S8*A*) (20). Moreover, because RHPs were recruited to the intermembrane spaces (Fig. 5*D*), the self-interacting 1a and RHP proteins (38) might cluster in the concave and convex membrane regions, respectively, neutralizing each other's induced membrane curvature to yield relatively flat sheets (Fig. S8*A*). Consistent with this possibility, absence of RHPs produced aberrant single layers with prominent, negatively curved bulges consistent with unbridled 1a-induced curvature (Fig. S8*B*).

Like excess 1a-interacting $2a^{Pol}$, GFP fusion to 1a-interacting RHPs inhibited spherule formation and induced membrane layer formation (Fig. S7). This phenotype is consistent with our independent findings that RHPs interact with 1a and localize to spherule and layer interiors (Figs. 4 and 5). As with $2a^{pol}$ (20), these effects may be due to steric issues or interference with competing 1a interactions, such as certain 1a–1a interactions.

RHPs also might contribute to RNA synthesis in ways beyond membrane shaping. By interacting with 1a, RHPs might modulate 1a conformation, multimerization, or membrane interaction to activate one or more 1a functions required for RNA synthesis, similar to membrane activation of Semliki Forest virus nsP1 capping functions (39). BMV RNA replication also requires high, balanced levels of lipid synthesis (40), many steps of which occur on RHP-stabilized tubular ER (25, 26, 34). However, deleting all three RHPs did not alter fatty acid levels or composition (Fig. S5). Moreover, although RHPs affect vesicular trafficking (41), deleting all three RHPs did not alter ER membrane localization of BMV RNA replication proteins 1a or $2a^{Pol}$ (Fig. S2). It remains possible that RHP deletion might alter the distribution of a host factor required for RNA replication.

Relation to Other (+)RNA Viruses. Several other membrane-associated host factors recently have been implicated in (+)RNA virus replication. BMV and poliovirus RNA replication depend on ER-localized Δ9 fatty acid desaturase Ole1p and secretory regulating factor GBF1, which is recruited to poliovirus RNA replication sites, although neither factor is required for replication-associated membrane rearrangements (40). Poliovirus also subverts membrane-rearranging autophagosomal pathways, with implications for RNA replication and virion release (42). Additionally, dominant-negative mutants of ESCRT-III proteins reduced tombusvirus RNA replication and the frequency of spherules in infected cells (43). Moreover, enterovirus 71 and poliovirus 2C proteins interact with human reticulon 3 (RTN3), and RTN3 knockdown decreased enterovirus 71 double-stranded RNA synthesis and protein expression (44). Although possible effects on membrane rearrangements were not determined, these results suggest that the BMV-RHP findings here may have implications for other (+)RNA viruses.

Overall, our data show that RHPs interact with BMV 1a and are essential for inducing and/or stabilizing the membrane rearrangements linked to BMV RNA replication. Further understanding of RPH roles in RNA replication by BMV and other viruses should provide additional insights into replication pathways and facilitate use of such host genes as potential targets for antiviral approaches.

Experimental Procedures

***S. cerevisiae* Strains and Plasmids.** The yeast strains used were as follows: YPH500 (MATα ura3–52 lys2–801 ade2–101 trp1-Δ63 his3-Δ200 leu2-Δ1), BY4741 (MATα his3Δ1 leu2Δ met15Δ ura3Δ), and NDY257 (BY471 rtn1::kanMX4 rtn2::kanMX4 yop1::kanMX4) (25). The following strains were generated for this work: RM1 (YPH500 rtn1::kanMX4), RM2 (YPH500 rtn2::kanMX4), RM3 (YPH500 yop1::kanMX4), RM4 (YPH500 rtn1::kanMX4 yop1::natMX4), and RM5 (YPH500 rtn2::trp1 yop1::KanMX4). Genomic insertions were made by using amplified KanMX4, NatMX4, or trp1 cassettes flanked by 5′ and 3′ homologous recombination regions. Strains expressing the chromosomal alleles of RTN1, RTN2, and YOP1 as GFP fusions were obtained from Invitrogen. For endogenous expression of the RHPs, the coding region of the full length protein plus the 300-bp upstream sequences were PCR-amplified from wt yeast DNA with appropriate primers and inserted into a CEN plasmid. A FLAG-tag was added at the C terminus of the RHPs. BMV 1a was expressed from the GAL1 promoter by using pB1YT3 (5), $2a^{pol}$ was expressed from pB2CT15 (ADH1 promoter) (14) or pB2YT5 (GAL1 promoter) (5), and BMV RNA3 was expressed from a CUP1 promoter using pB3VG128His, a pB3MS82 derivative (5). Plasmids encoding Sec63-GFP (pJK59) (20), free GFP, and $2a^{pol}$-GFP (8) have been described. Plasmid transformation and yeast cultivation were performed as described (14).

RNA and Protein Analysis. RNA isolation, Northern and Western blot analysis, and anti-1a and anti-Pgk1 antibodies were as described (8, 14). Anti-FLAG and anti-GFP mouse polyclonal antibodies were purchased from Sigma and Molecular Probes, respectively.

Coimmunoprecipitation. Yeast cells were lysed in RIPA buffer (1% Nonidet P-40, 0.1% SDS, 50 mM Tris at pH 8.0, 150 mM NaCl, 0.5% sodium deoxycholate, 5 mM EDTA, 10 mM NaF, 10 mM NaPPi, 2 mM phenylmethylsulfonyl, 5 mM benzamidine, and 10 μg/mL each of chymostatin, pepstatin A, leupeptin, and bestatin) by using glass beads and a bead beater, and the supernatant was collected after centrifugation. For immunoprecipitation, yeast lysates were mixed with Protein A Sepharose beads (GE Healthcare) and anti-1a, anti-FLAG, or anti-GFP antibodies overnight at 4 °C. Beads were pelleted and washed with RIPA buffer before boiling in 1× SDS gel loading buffer and running samples in 4–15% SDS/PAGE gels.

Confocal Laser Microscopy. To detect the subcellular localization of BMV proteins in RHP deletion strains, yeast were transformed with plasmids expressing 1a and $2a^{pol}$ and Sec63-GFP. To detect the localization of RHPs, FLAG-tagged RHPs or strains expressing GFP fusions to the chromosomal alleles of *RTN1*, *RTN2*, and *YOP1* were transformed with empty plasmids or plasmids encoding 1a and $2a^{pol}$. Confocal microscopy was performed on a Bio-Rad 1024 double-channel confocal microscope as described (12).

Electron Microscopy. Conventional and immunolabeling fixation EM was done as described (15). For immunogold labeling, the percentage of relocalized RHPs was calculated by comparing the number of gold particles in or near the perinuclear ER in the absence versus the presence of 1a. Background labeling was determined by using cells lacking FLAG-tagged RHPs. Specific labeling was determined by subtracting the background labeling density. The diameter of >50 spherules was measured with the imaging program ITEM Analysis (Soft Imaging Systems). For additional information, see *SI Experimental Procedures*.

ACKNOWLEDGMENTS. We thank Benjamin August and Randall Massey of the University of Wisconsin Medical School Electron Microscopy Facility for assistance with EM, Lance Rodenkirch of the W. M. Keck Laboratory for Biological Imaging for assistance with confocal microscopy, and Dr. William Prinz (the National Institutes of Health, Bethesda, MD) for providing the triple-knockout strain. This project was supported by National Institutes of Health Grant GM35072. P.A. is a Howard Hughes Medical Institute investigator. A.D. was supported by National Institutes of Health Predoctoral Grant T32 GM07215.

1. Miller S, Krijnse-Locker J (2008) Modification of intracellular membrane structures for virus replication. *Nat Rev Microbiol* 6:363–374.

2. Knoops K, et al. (2008) SARS-coronavirus replication is supported by a reticulovesicular network of modified endoplasmic reticulum. *PLoS Biol* 6:e226.

3. Kopek BG, Perkins G, Miller DJ, Ellisman MH, Ahlquist P (2007) Three-dimensional analysis of a viral RNA replication complex reveals a virus-induced mini-organelle. *PLoS Biol* 5:e220.
4. Ahola T, Ahlquist P (1999) Putative RNA capping activities encoded by brome mosaic virus: Methylation and covalent binding of guanylate by replicase protein 1a. *J Virol* 73:10061–10069.
5. Ahola T, den Boon JA, Ahlquist P (2000) Helicase and capping enzyme active site mutations in brome mosaic virus protein 1a cause defects in template recruitment, negative-strand RNA synthesis, and viral RNA capping. *J Virol* 74:8803–8811.
6. Kong F, Sivakumaran K, Kao C (1999) The N-terminal half of the brome mosaic virus 1a protein has RNA capping-associated activities: Specificity for GTP and S-adenosylmethionine. *Virology* 259:200–210.
7. Wang X, et al. (2005) Brome mosaic virus 1a nucleoside triphosphatase/helicase domain plays crucial roles in recruiting RNA replication templates. *J Virol* 79:13747–13758.
8. Chen J, Ahlquist P (2000) Brome mosaic virus polymerase-like protein 2a is directed to the endoplasmic reticulum by helicase-like viral protein 1a. *J Virol* 74:4310–4318.
9. Kao CC, Ahlquist P (1992) Identification of the domains required for direct interaction of the helicase-like and polymerase-like RNA replication proteins of brome mosaic virus. *J Virol* 66:7293–7302.
10. Krol MA, et al. (1999) RNA-controlled polymorphism in the in vivo assembly of 180-subunit and 120-subunit virions from a single capsid protein. *Proc Natl Acad Sci USA* 96:13650–13655.
11. Sullivan ML, Ahlquist P (1999) A brome mosaic virus intergenic RNA3 replication signal functions with viral replication protein 1a to dramatically stabilize RNA in vivo. *J Virol* 73:2622–2632.
12. Restrepo-Hartwig M, Ahlquist P (1999) Brome mosaic virus RNA replication proteins 1a and 2a colocalize and 1a independently localizes on the yeast endoplasmic reticulum. *J Virol* 73:10303–10309.
13. Restrepo-Hartwig MA, Ahlquist P (1996) Brome mosaic virus helicase- and polymerase-like proteins colocalize on the endoplasmic reticulum at sites of viral RNA synthesis. *J Virol* 70:8908–8916.
14. Janda M, Ahlquist P (1993) RNA-dependent replication, transcription, and persistence of brome mosaic virus RNA replicons in S. cerevisiae. *Cell* 72:961–970.
15. Schwartz M, et al. (2002) A positive-strand RNA virus replication complex parallels form and function of retrovirus capsids. *Mol Cell* 9:505–514.
16. den Boon JA, Chen J, Ahlquist P (2001) Identification of sequences in Brome mosaic virus replicase protein 1a that mediate association with endoplasmic reticulum membranes. *J Virol* 75:12370–12381.
17. O'Reilly EK, Kao CC (1998) Analysis of RNA-dependent RNA polymerase structure and function as guided by known polymerase structures and computer predictions of secondary structure. *Virology* 252:287–303.
18. Welsch S, et al. (2009) Composition and three-dimensional architecture of the dengue virus replication and assembly sites. *Cell Host Microbe* 5:365–375.
19. Kujala P, et al. (2001) Biogenesis of the Semliki Forest virus RNA replication complex. *J Virol* 75:3873–3884.
20. Schwartz M, Chen J, Lee WM, Janda M, Ahlquist P (2004) Alternate, virus-induced membrane rearrangements support positive-strand RNA virus genome replication. *Proc Natl Acad Sci USA* 101:11263–11268.
21. Yang YS, Strittmatter SM (2007) The reticulons: A family of proteins with diverse functions. *Genome Biol* 8:234.
22. Nziengui H, Schoefs B (2009) Functions of reticulons in plants: What we can learn from animals and yeasts. *Cell Mol Life Sci* 66:584–595.
23. Audhya A, Desai A, Oegema K (2007) A role for Rab5 in structuring the endoplasmic reticulum. *J Cell Biol* 178:43–56.
24. Wakefield S, Tear G (2006) The Drosophila reticulon, Rtnl-1, has multiple differentially expressed isoforms that are associated with a sub-compartment of the endoplasmic reticulum. *Cell Mol Life Sci* 63:2027–2038.
25. Voeltz GK, Prinz WA, Shibata Y, Rist JM, Rapoport TA (2006) A class of membrane proteins shaping the tubular endoplasmic reticulum. *Cell* 124:573–586.
26. De Craene JO, et al. (2006) Rtn1p is involved in structuring the cortical endoplasmic reticulum. *Mol Biol Cell* 17:3009–3020.
27. Kiseleva E, Morozova KN, Voeltz GK, Allen TD, Goldberg MW (2007) Reticulon 4a/NogoA locates to regions of high membrane curvature and may have a role in nuclear envelope growth. *J Struct Biol* 160:224–235.
28. Tolley N, et al. (2008) Overexpression of a plant reticulon remodels the lumen of the cortical endoplasmic reticulum but does not perturb protein transport. *Traffic* 9: 94–102.
29. Kushner DB, et al. (2003) Systematic, genome-wide identification of host genes affecting replication of a positive-strand RNA virus. *Proc Natl Acad Sci USA* 100: 15764–15769.
30. Ghaemmaghami S, et al. (2003) Global analysis of protein expression in yeast. *Nature* 425:737–741.
31. Liu L, et al. (2009) An amphipathic alpha-helix controls multiple roles of brome mosaic virus protein 1a in RNA replication complex assembly and function. *PLoS Pathog* 5: e1000351.
32. Noueiry AO, Diez J, Falk SP, Chen J, Ahlquist P (2003) Yeast Lsm1p-7p/Pat1p deadenylation-dependent mRNA-decapping factors are required for brome mosaic virus genomic RNA translation. *Mol Cell Biol* 23:4094–4106.
33. Janda M, Ahlquist P (1998) Brome mosaic virus RNA replication protein 1a dramatically increases in vivo stability but not translation of viral genomic RNA3. *Proc Natl Acad Sci USA* 95:2227–2232.
34. Baumann O, Walz B (2001) Endoplasmic reticulum of animal cells and its organization into structural and functional domains. *Int Rev Cytol* 205:149–214.
35. Hu J, et al. (2008) Membrane proteins of the endoplasmic reticulum induce high-curvature tubules. *Science* 319:1247–1250.
36. Prinz WA, et al. (2000) Mutants affecting the structure of the cortical endoplasmic reticulum in Saccharomyces cerevisiae. *J Cell Biol* 150:461–474.
37. Hayat MA (1991) *Colloidal Gold* (Academic, San Diego).
38. Shibata Y, et al. (2008) The reticulon and DP1/Yop1p proteins form immobile oligomers in the tubular endoplasmic reticulum. *J Biol Chem* 283:18892–18904.
39. Ahola T, Lampio A, Auvinen P, Kääriäinen L (1999) Semliki Forest virus mRNA capping enzyme requires association with anionic membrane phospholipids for activity. *EMBO J* 18:3164–3172.
40. Lee WM, Ahlquist P (2003) Membrane synthesis, specific lipid requirements, and localized lipid composition changes associated with a positive-strand RNA virus RNA replication protein. *J Virol* 77:12819–12828.
41. Steiner P, et al. (2004) Reticulon 1-C/neuroendocrine-specific protein-C interacts with SNARE proteins. *J Neurochem* 89:569–580.
42. Taylor MP, Burgon TB, Kirkegaard K, Jackson WT (2009) Role of microtubules in extracellular release of poliovirus. *J Virol* 83:6599–6609.
43. Barajas D, Jiang Y, Nagy PD (2009) A unique role for the host ESCRT proteins in replication of Tomato bushy stunt virus. *PLoS Pathog* 5:e1000705.
44. Tang WF, et al. (2007) Reticulon 3 binds the 2C protein of enterovirus 71 and is required for viral replication. *J Biol Chem* 282:5888–5898.